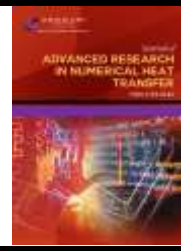




Journal of Advanced Research in Numerical Heat Transfer

Journal homepage:
<https://semarakilmu.com.my/journals/index.php/arnht/index>
ISSN: 2735-0142



Thermal Performance Improvement of Microchannel Heat Sink for Electronic Device Cooling System Using Numerical Analysis

Muhammad Aidil Safwan Abdul Aziz¹, Nofrizalidris Darlis^{2,*}, Izuan Amin Ishak¹, Nor Atiqah Zolpakar³, Mohammad Arafat¹, Muhammadu Masin Muhammadu⁴

¹ Department of Mechanical Engineering Technology, Faculty of Engineering Technology, Universiti Tun Hussein Onn Malaysia, 84600 Pagoh, Johor, Malaysia, Malaysia

² Centre of Automotive and Powertrain Technology, Faculty of Engineering Technology, Universiti Tun Hussein Onn Malaysia, 84600 Pagoh, Johor, Malaysia, Malaysia

³ Faculty of Mechanical & Automotive Engineering Technology, Universiti Malaysia Pahang, 26600 Pekan, Pahang, Malaysia

⁴ Department of Mechanical Engineering, Federal University of Technology, Minna, Nigeria

ARTICLE INFO

Article history:

Received 24 August 2024

Received in revised form 27 September 2024

Accepted 25 October 2024

Available online 30 November 2024

Keywords:

Microchannel heat sink (MCHS); Thermal performance; Pin-fin configuration; CFD simulation; Heat transfer optimization

ABSTRACT

The increasing miniaturization of technology has intensified thermal challenges, particularly concerning the cooling of small components like integrated circuits and personal computer. In order to guarantee the safety and extended operation of these devices, the thermal performance must be looked into with the purpose of dissipating them. One of the most common solutions is a microchannel heat sink (MCHS) because of its inherent property of a higher surface area-to-volume ratio. Microchannel heat sinks offer a common solution, but optimizing their configurations remains a subject of interest especially when incorporating multiple thermal enhancing methods within a microchannel heat sink. The objectives of the study is to analyse the effects of varying pin-fin geometries on key thermal performance metrics, such as maximum temperature and pressure drop, and also observing and comparing the streamline patterns generated within the cross flow microchannel heat sink. Computational Fluid Dynamics (CFD) simulations were conducted using Ansys to evaluate the thermal performance of different pin-fin geometries and also capture the streamlines pattern generated from the studied geometry of the pin fin. The results indicate that hexagon-shaped pin-fins reduced the maximum temperature by 1 to 3 Kelvin compared to the base model with circular pin-fins. However, while the circular pin-fins produced the lowest pressure drop, the hexagon-shaped pin-fins had the second-highest pressure drop among the geometries studied. This proves the significance of geometry selection for the pin fin as it affected the thermal performance of the microchannel heat sink with cross flow effects.

1. Introduction

As time moves, miniaturizing the integrated circuit (IC) has been the trend and fitting multiple different components lead to thermal issues which could potentially worsen the efficiency of the

* Corresponding author.

E-mail address: nofrizal@uthm.edu.my (Nofrizalidris Darlis)

<https://doi.org/10.37934/arnht.26.1.8498>

performance or even worse damaging the whole IC, which were mentioned within multiple past studies [1-3]. So thermal management of IC is crucial when designing any electrical components especially since it is presence in a wide variety of electrical components for example, smartphones, smart televisions, solar panel systems, computers and many more. On the other hand, the internet's recent rapid development necessitates personal computer (PC) capability that can handle larger data sets more quickly. High-performance PC built-in devices have been created to satisfy this need. CPU exhibits a competitive release of faster products and a move towards smaller, more elegant designs. Abbas *et al.*, also mentioned in their study that this leads to higher heat density and increased heat dissipation, making CPU temperature rise and causing the shortened life, malfunction, and failure of CPU [4].

It was mentioned within past study conducted by Japar *et al.*, [5] that an improved cooling method called microchannel heat sink (MCHS) is used to meet the cooling needs of electronic devices that have high-power integrated circuit packages (microchips) installed. A variety of innovative microchannel designs have been developed to enhance an MCHS's heat transmission capability. Microscale-sized fluid flow channels are combined into microchannel heat sinks. These are employed to disperse large heat fluxes from heat sources with high power density in constrained areas. Numerous cooling applications call for the use of micro-channel heat sinks, such as the cooling of computer components (CPUs, GPUs, memory storage devices, etc.), high-powered electronic components (IGBTs), proton exchange membrane fuel cells, laser diode arrays, combustors, and the evaporator/condenser in a miniature refrigerator. One of the main fields of use for MCHS is thermal management in electronics, as noted in previous studies [6].

The substantial heat flux cooling that can be achieved with the microchannel heat sink makes it a popular heat transfer technology. Nevertheless, there are several drawbacks to conventional microchannel heat sinks, including high wall superheat, low boiling critical heat flow, high pressure drops, and inconsistent temperature. Consequently, many researchers have carried out studies in designing and improving it to further improve their comprehensive heat transfer performance, as noted in previous research [7]. There are a lot of configurations that can be made in designing a microchannel heat sink (depending on the purpose for the microchannel heat sink to serve) that was mentioned in numerous past studies [7-9], for example, the layout of the microchannel, the structure of the microchannel wall, the position of the inlet and outlet, the material types, the surface treatment and many more.

Internal enhancement techniques, such as utilizing ribs and pin-fin configurations, are employed to improve the thermal performance of a microchannel heat sink. This method aims to improve the heat sink's ability to dissipate heat by using pin the added structure within the microchannel heat sink. A previous study that was conducted by Loon *et al.*, [10] gathered that with the addition of rectangular ribs, it can significantly increase the thermal performance of a heat sink by providing secondary and tertiary channels within the microchannels of the heat sink. The novel heat sink design, with secondary channels, tertiary channels and rectangular ribs studied yielded the largest convective heat transfer surface area as compared to other studied microchannel.

A review paper wrote by Dong *et al.*, [11] mentioned that, with the addition of a fin to MCHS has the potential to considerably boost the heat transfer surface area, leading to improved heat transfer efficiency. Multiple studies have shown that different geometry of the pin fin used will yield different results. Ahmadian-Elmi M *et al.*, [12] carried out research in optimizing the pin fin configuration by using the number of fins, the fin height, the fin diameter and the transverse pitch. The results gathered were, increasing the number and diameter of the fin will lead to an increase in pressure drop and heat transfer coefficient while increasing the fin height and transverse pitch results in the complete opposite.

Another study conducted by Ndao *et al.*, [13] using circular, hydrofoil, square and elliptical pin fin in a microchannel to analyze the heat transfer coefficient and the effect of cross flow. The result shows circular that circular pin fin has the best heat transfer coefficient followed with square pin fin. The study discovered that cross flow effects had little to no effect towards the heat transfer coefficient when varying the diameter of the circular pin fin.

This study addresses a critical gap in the existing research by focusing on the influence of different pin-fin geometries within a cross flow microchannel heat sink, a design previously studied but not thoroughly explored in terms of geometric variation. While past studies have demonstrated the thermal benefits of cross flow designs, the specific impact of varying pin-fin geometries on thermal performance such as maximum temperature, pressure drop, and streamline patterns, remains underexplored. This research provides deeper insights into optimizing heat sink designs by addressing this gap. It is noted that the geometry of the pin fin can affect the thermal performance of the heat sink thus varying the geometry of the pin fin can help in further improving the heat sink performance. Therefore, numerical simulations using computational fluid dynamics will be used to investigate the impact of varying the geometry of the pin fin of the heat sink under different Reynolds numbers. The Reynolds number used starts from 200-1000 with 100 increments whereas the geometry of the pin studied was square, hexagon and rhombus.

2. Methodology

2.1 Research Framework

Computational Fluid Dynamic (CFD) analysis was used to carry out the current investigation. SolidWorks software was used to design the base model of the microchannel heat sink alongside the different geometry of the pin fin that will be studied. The ANSYS Fluent module generates the meshing and computational domain for simulation after the geometry modelling is finished. Next, the grid independence test and a comparison of the simulation results with the reference paper start the validation process. The model with proposed geometry of the pin fin will be run under different Reynolds numbers and compared between them to identify the heat sink with the highest thermal performance.

2.2 MCHS Model

The base model used in this study is based on the past studied conducted by Rao *et al.*, [14] where the pin fin configuration located at the middle of the heat sink was changed to proposed geometry that is square, hexagon and rhombus. Figure 1(a), (b) and (c) shows the microchannel heat sink model that was recreated using SolidWorks software. The model was used as the base model where the geometry of the pin fin was cylindrical. Figure 1(d) shows the pin fin configuration that was used as the base model and will be configured into different geometries. The purpose of the hotspot configuration was to eliminate hotspot effects that were simulated through having different heat fluxes at the bottom of the heat sink.

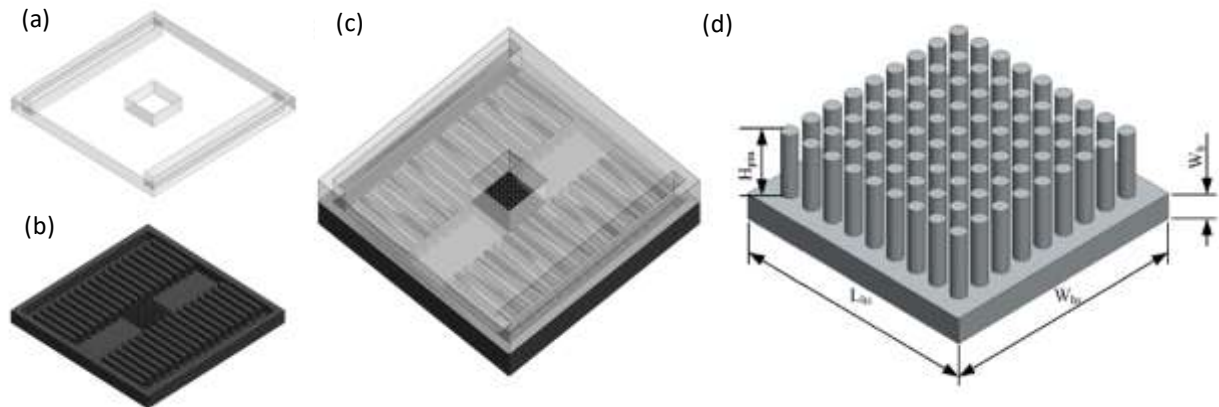


Fig. 1. (a) top cover of the heat sink (b) base model of the microchannel heat sink (c) isometric view of the microchannel heat sink with the cover (d) pin fin configuration for the base model of the microchannel heat sink

2.3 Proposed Design

The proposed geometry of the pin fin includes square, hexagon, and rhombus, as previous studies [15,16] have shown that these shapes exhibit the highest thermal performance. The dimensions of the pin fin for the proposed geometry were configured whereas the spacing in between the pin fin was kept the same. Bhandari *et al.*, [15] conducted a study where they varied the radius of the pin fin, and the results showed that the thermal performance will increase as the radius goes up to 0.275mm then decrease after it exceeds it. By using the same radius to spacing ratio, the proposed design of the pin was set to 73.333 micrometer. Figure 2 shows the proposed geometry of the pin fin with different points of views.

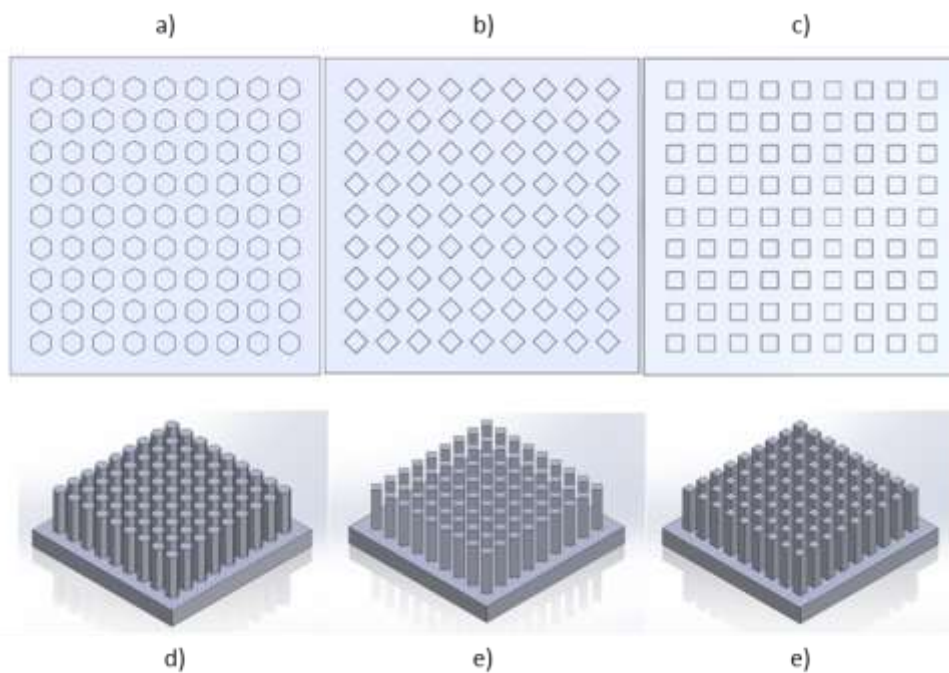


Fig. 2. (a) top view of hexagon-shaped pin fin (b) top view of rhombus-shaped pin fin (c) top view of square-shaped pin fin (d) isometric view of hexagon-shaped pin fin (e) isometric view of rhombus-shaped pin fin (f) isometric view of square-shaped pin fin

2.4 Boundary Conditions

Another domain is constructed to mimic the fluid passing within the heat sink where it will fill up the hollow part between the glass cover and the heat sink. The glass cover was then suppressed as it was not required for the study leaving out only 2 domains, that is the heat sink (solid domain), and the fluid domain created as can be seen in Figure 3. To ease the computational load, only a quarter of the heat sink model was used within the simulation. The model's boundary condition such as the inlet velocity, outlet velocity, symmetry wall and heat flux were established. Figure 4 shows the boundary conditions set up for the simulation where the inlet, the outlet, and the symmetry walls are located followed with Figure 5 that shows the bottom view of the heat sink having both the hotspot (smaller square) and the background (larger square) that will be having different heat flux.

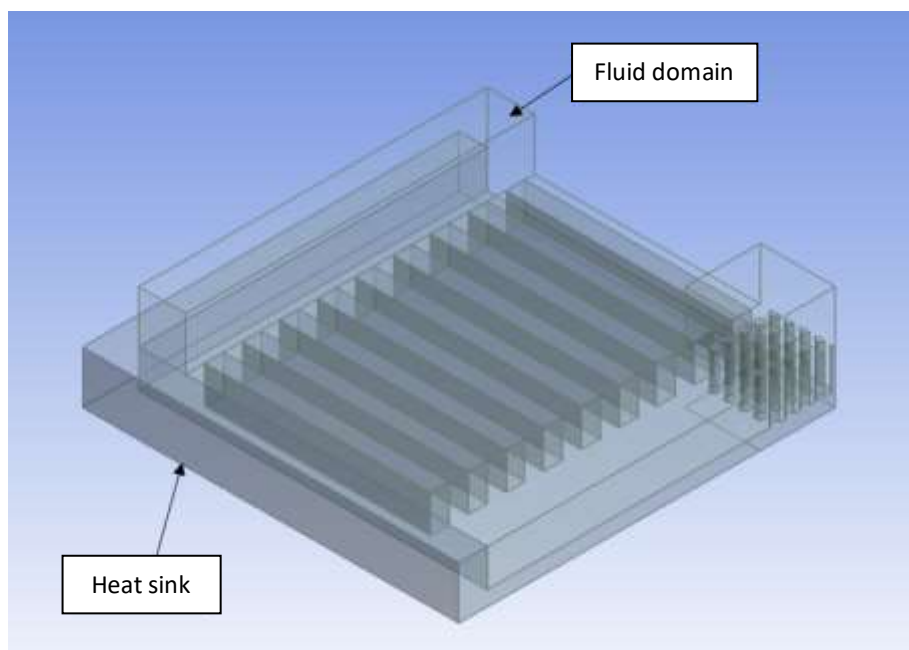


Fig. 3. Different domain that was used within the simulation that is fluid domain and solid domain (that is the heat sink body)

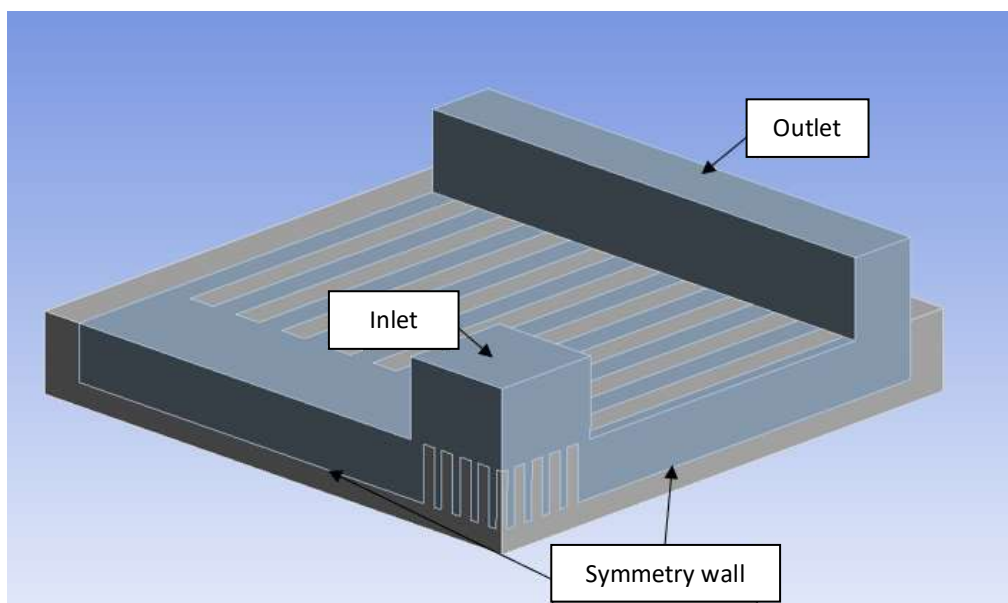


Fig. 4. Isometric view of the heat sink and fluid domain

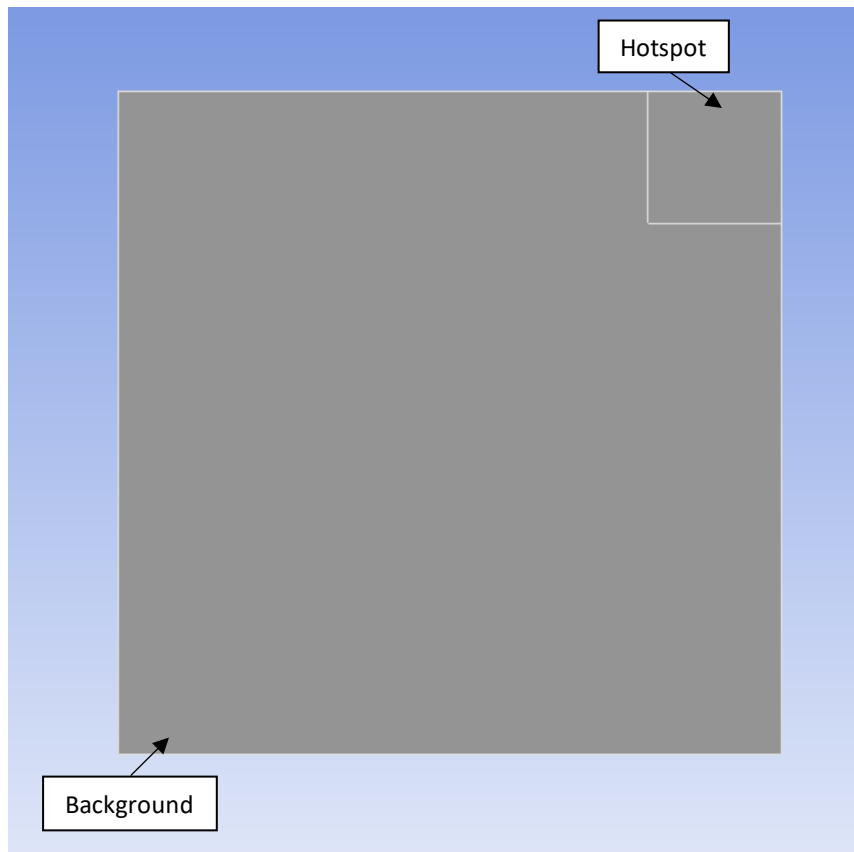


Fig. 5. (a) Bottom view of the heat sink

Given the simulation was run with different Reynolds number, the inlet velocity was calculated using Eq. (1) where ρ_f is the fluid density and μ_f is the dynamic viscosity, both calculated through the thermophysical property, D_h is the hydraulic density, and Re is the Reynolds number used for this study which ranges from 200-1000. Table 1 shows the inlet velocity for different Reynolds numbers followed with Table 2 that shows the other details and values of the boundary condition.

$$Re = \frac{\rho_f v_{avg} D_h}{\mu_f} \quad (1)$$

Table 1
 Inlet velocity according to the Reynolds number

| Reynolds number | Inlet velocity (m/s) |
|-----------------|----------------------|
| 200 | 0.6029 |
| 300 | 0.9043 |
| 400 | 1.2058 |
| 500 | 1.5072 |
| 600 | 1.8087 |
| 700 | 2.1101 |
| 800 | 2.4115 |
| 900 | 2.7130 |
| 1000 | 3.0144 |

Table 2
 Details and values of the boundary conditions used

| Details | Boundary conditions | Values |
|----------------|--|-------------------------------|
| Inlet | Inlet velocity | Table 1 |
| Inlet | Temperature | 300 K |
| Outlet | Outlet pressure | 0 Pa |
| Symmetry wall | Wall boundary | Stationary |
| Hotspot | Heat flux | 300 W/cm ² |
| Background | Heat flux | 50 W/cm ² |
| Contact Region | Contact between fluid domain and heat sink | No slip and coupled interface |

2.5 Grid Independence Test

For numerical analysis, the CFD model's target space is split up into a limited number of grids. For this reason, the best possible grid design is needed to produce accurate findings. It was mentioned in previous study [17] that generally, the grid independence test is conducted to create an ideal grid for the simulation. The ANSYS Meshing feature was utilized to create meshes for the model that consist of the heat sink and the fluid domain. Not only that, since the pin fin configuration is significantly smaller than the heat sink and fluid domain, but the surface of the pin fin was also meshed using different sizes. Table 3 shows the parts of the model that change in size starting from M1 up to M4. The size of the meshing is halved from M1 to M2 and continues the pattern up to M4. This will result in a different total number of elements where it shows, as the sizes of the mesh decrease, the total number of elements will increase.

The results of the maximum temperature gathered from the simulation for each of the mesh sizes were then plotted out as shown in Figure 6. It was observed that the results differ for each of the meshes. As the mesh sizes progress from M1 to M4, the percentage of difference also decreases. The percentage difference between M2 to M3 has already reached less than 1% difference as it was not achieved between M1 to M2. M3 was chosen as the element size of this study even though the percentage difference between M3 to M4 has even lower percentage. This is because the percentage difference between M2 and M3 is already lower than 1% and to decrease the computational load for the simulation to be run as smaller mesh sizes will lead to higher number of elements which results in increase of time for the simulation to be completed.

Table 3
 Details and values of different mesh sizes

| Details | M1 | M2 | M3 | M4 |
|-----------------------------------|--------|--------|--------|---------|
| Heat sink (μm) | 400 | 200 | 100 | 50 |
| Fluid domain (μm) | 400 | 200 | 100 | 50 |
| Pin fin surface (μm) | 25 | 25 | 25 | 25 |
| Number of elements | 268155 | 286914 | 429831 | 1581502 |
| Maximum temperature (K) | 335.39 | 327.96 | 327.40 | 327.16 |
| Percentage difference (%) | | 2.217 | 0.169 | 0.0763 |

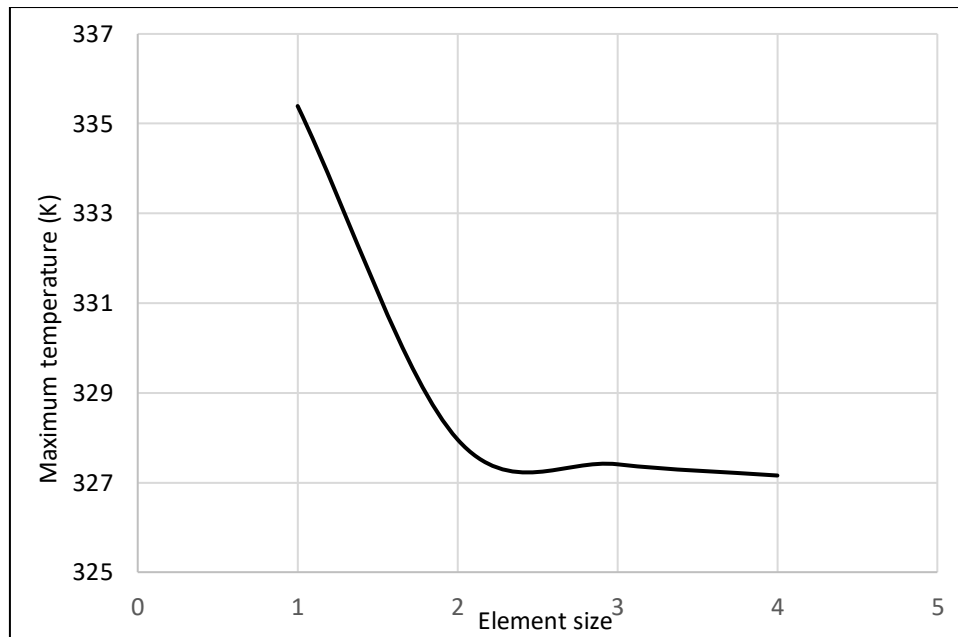


Fig. 6. Grid independence test based on the Reynolds number of 200

2.5 CFD validation

The circular pin fin, that is the base model used within the study, was validated using the same exact model that was studied by Rao *et al.*, with similar simulations setup. The only distinct difference is that the past study utilized Deionized Water with its own thermophysical parameters which requires User Defined Functions (UDF). Instead, the current study uses two different coolant that is Water and Deionized Water that does not require UDF which is achieved through substituting 300K (inlet temperature) within the thermophysical parameters to obtain the exact values. Figure 7 shows the maximum temperature results gathered from the current simulation, compared to the past results. This demonstrates that the model used within the current study is appropriate for further simulation using proposed geometry of pin fin regardless of the type of coolant used. This is simply because the percentage of error across the Reynolds number between the past and current results of maximum temperature shows less than 4% of error for both types of coolant as shown in Figure 7. Most significant difference can be observed at Reynolds number 200 where the percentage of error for both Water and Deionized Water at its highest that is 3.34% and 3.06% respectively. Hence, the result for the current study is validated due to its percentage of errors are within the acceptable ranges across all the Reynolds numbers used for this study.

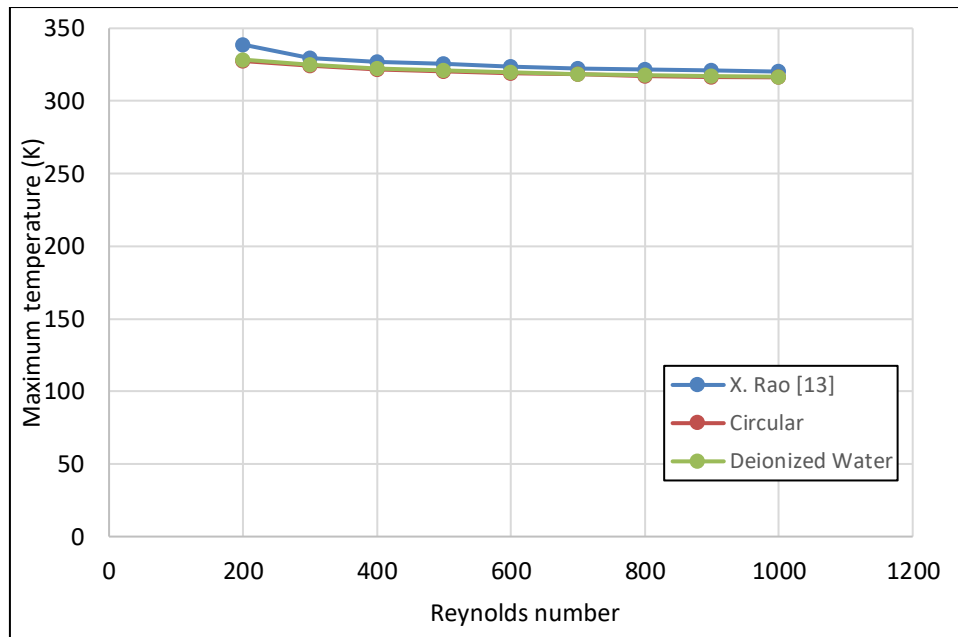


Fig. 7. Comparison of the results of maximum temperature between the past and current study

3. Thermal Performance Analysis

3.1 Maximum Temperature

Figure 8 shows the graph plotted from the results for maximum temperature gathered across the geometry of the pin fin across different Reynolds numbers. It is observed that the trend of the maximum temperature across all the different geometry decreases as the Reynolds number increases where, hexagon shaped pin fin yields the lowest amongst the other pin fin studied. This shows that hexagon shaped pin fin design can effectively suppress temperature rises in the hotspot area compared to the other geometry. Compared to the previous study [14] with the same model of microchannel heat sink which utilized circular, hexagonal pin fin's yield lower maximum temperature by about 1-3 Kelvin across all of the Reynolds number that was used in the study.

Notably, as the Reynolds number increase, the base model that has circular shaped pin fin was able to minimize the advantages that hexagon shaped pin fin has over it as the Reynolds number increases to 1000 despite circular having the highest maximum temperature at 200 Reynolds number. Circular shaped pin fin shows great results as the Reynolds number increases as it was able to lower the maximum temperature and perform better compared to square and rhombus starting from 500 Reynolds number.

The difference of boundary layer effect also affects the results of the maximum temperature where it is presence on all the geometry but, the significant of it is where it should be focused on. For the circular shaped pin fin, the boundary layer seems to be more pronounced as the Reynolds number increases thus further lowering the maximum temperature surpassing both square and rhombus shaped pin fin. Despite the good performance of the circular pin fin, hexagon shaped pin fin maintains superior performance across all the Reynolds numbers showing the lowest maximum temperature amongst all the proposed geometry and the base model. This shows that hexagon shaped pin fin inherently promotes the highest heat transfer compared to the other studied geometry.

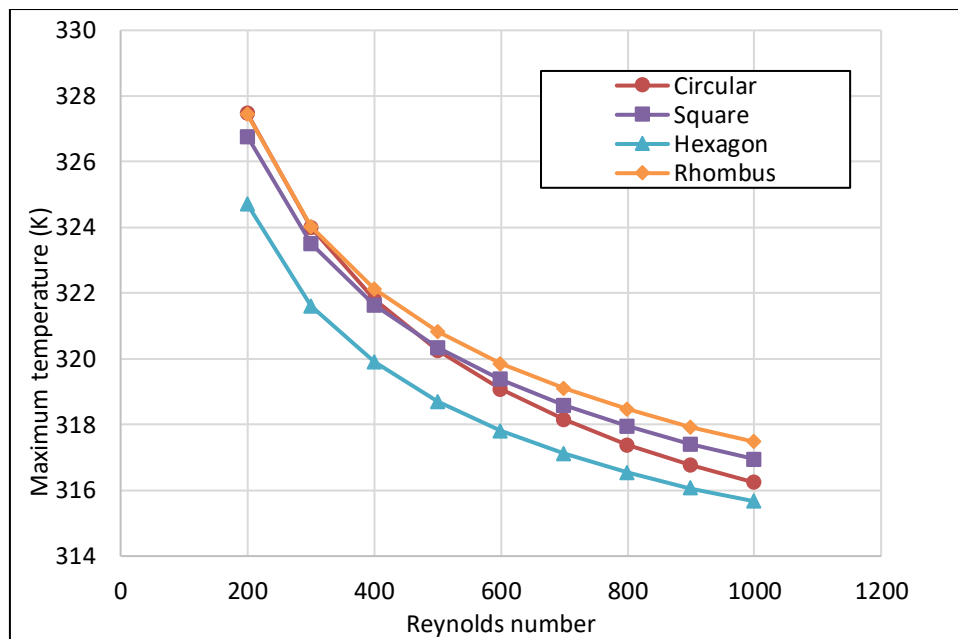


Fig. 8. Graph of maximum temperature against Reynolds number across proposed geometry

3.2 Pressure Drop

The relationship between the Reynolds number and pressure drop for various pin fin designs inside the microchannel heat sink is shown in the graph. Due to increased flow resistance, the graph shown in Figure 9 indicates that for all tested geometries, the pressure drop increases as the Reynolds number. This result agrees with previous study conducted by past researchers such as Qiu *et al.*, [18] and Guan *et al.*, [19] where they also observe the impact of studied parameters to the pressure drop yield, where the results gathered shows that pressure drop will increase as Reynolds number increase. When examining the pin fin's geometry, the base model, which employs a circular pin fin, yields the lowest pressure drop of all the suggested shapes, implying that it has the least amount of resistance to fluid flow.

The second lowest pressure drop was generated by square shaped pin fin. The highest-pressure drop was yielded by rhombus shaped pin fin which was followed closely by the hexagon shaped pin fin despite it having the lowest maximum temperature amongst all the studied geometry of pin fin. Results indicate that streamline-shaped pin fins have less pressure drop than other sharp-edged geometries; circular-shaped pin fins have the least pressure drop when compared to square, hexagonal, and rhombus-shaped pin fin.

Although the hexagon-shaped pin-fin achieved the lowest maximum temperature among all the geometries studied, it has the drawback of a relatively high pressure drop. Compared to findings from the previous study [14], which used circular pin-fins, the hexagon-shaped pin-fin resulted in nearly 60% higher pressure drop, despite maintaining lower temperatures than those observed in the earlier study. This highlights the trade-off between enhanced thermal performance and increased pressure drop in the design.

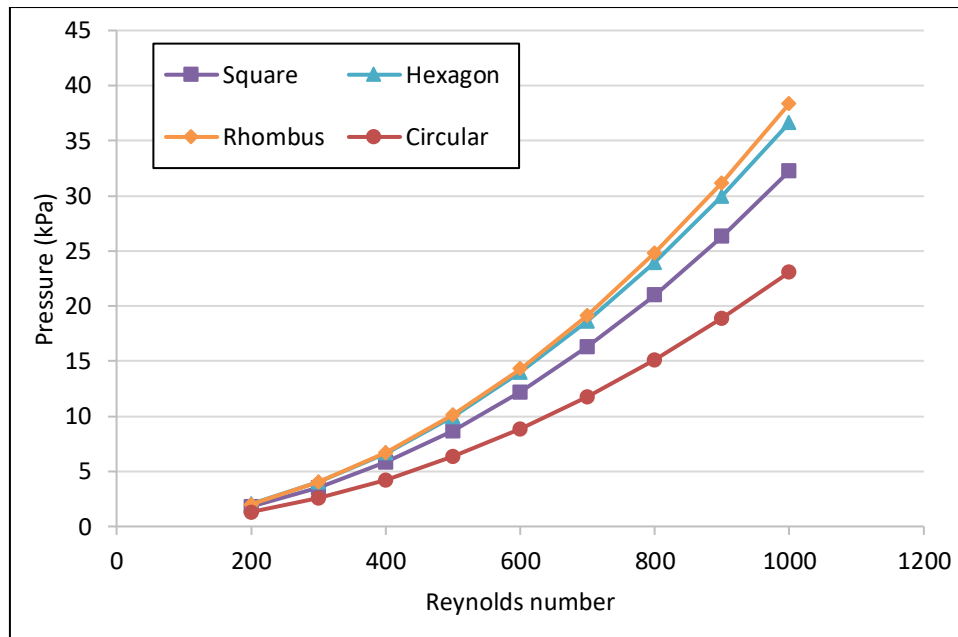


Fig. 9. Graph of pressure drop against Reynolds number across proposed geometry

3.3 Streamline

3.3.1 Circular (Base model)

The flow generated from the circle shaped pin fin shows that it is streamlined on both Reynolds numbers (200 and 1000) as shown in Figure 10. This translates to the lowest pressure drop yielded compared to the other proposed geometry of pin fin as the flow faces less resistance and fewer obstructions. The clear difference besides the velocity contours is that the formation of vortices at the wake region are more prominent at the higher Reynolds number. The presence of vortices helps in further improving the heat transfer as it promotes fluid mixing whilst still maintaining a low pressure drop. This is proven from the maximum temperature results gathered where it managed to achieve lower temperature compared to square and rhombus shaped pin fin as the Reynolds number increase.

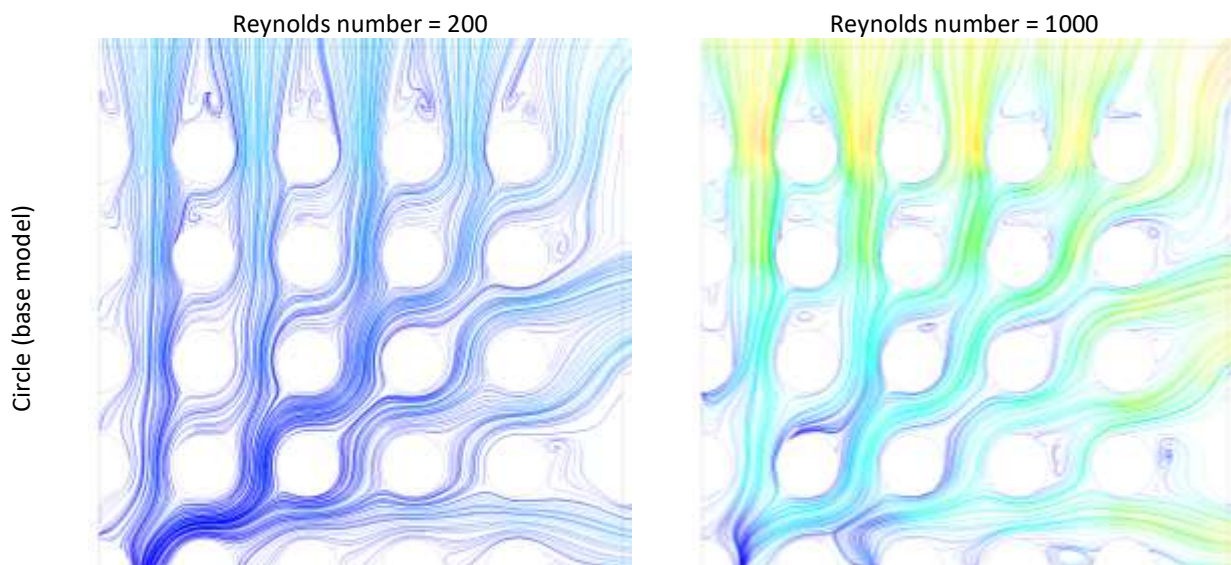


Fig. 10. Streamlines results gathered for circular shaped pin fin at Reynolds number 200 and 1000

3.3.2 Square

The same trend can be observed for the square shaped pin fin as it also shows uniform distribution around the pin fin and streamlined flow, but it differs in terms of the vortices formed at the wake region. There are fewer vortices generated within circular shaped pin fin as compared to the square shaped pin fin. This has caused the square shaped pin to have a higher pressure drop than the circular shaped pin especially at Reynolds number 1000 where the vortices formed are more prominent within square shaped pin fin as can be seen in Figure 11. This translates to the pressure drop recorded where square shaped pin fin yields higher pressure drop compared to circular shaped pin fin.

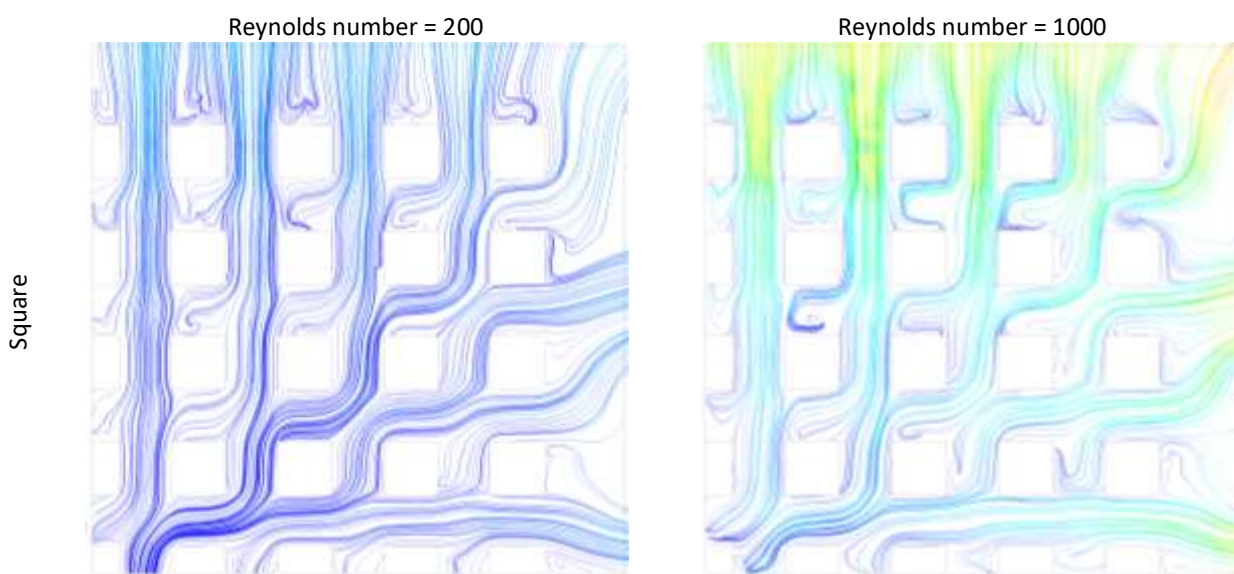


Fig. 11. Streamlines results gathered for square shaped pin fin at Reynolds number 200 and 1000

3.3.3 Rhombus

The rhombus shaped pin fin shows a more prominent vortex formation especially at 1000 Reynolds number, as shown in Figure 12. This configuration shows non-uniform flow streamlines with a notable degree of clustering and more turbulent flow. The non-uniform flow patterns shown by this clustering of streamlines have a noticeable impact on the pressure drop. The combination of prominent vortex production and non-uniform streamlines results in the biggest pressure drop among the studied geometries, with rhombus shaped pin fins yielding the highest pressure drop as shown in Figure 12.

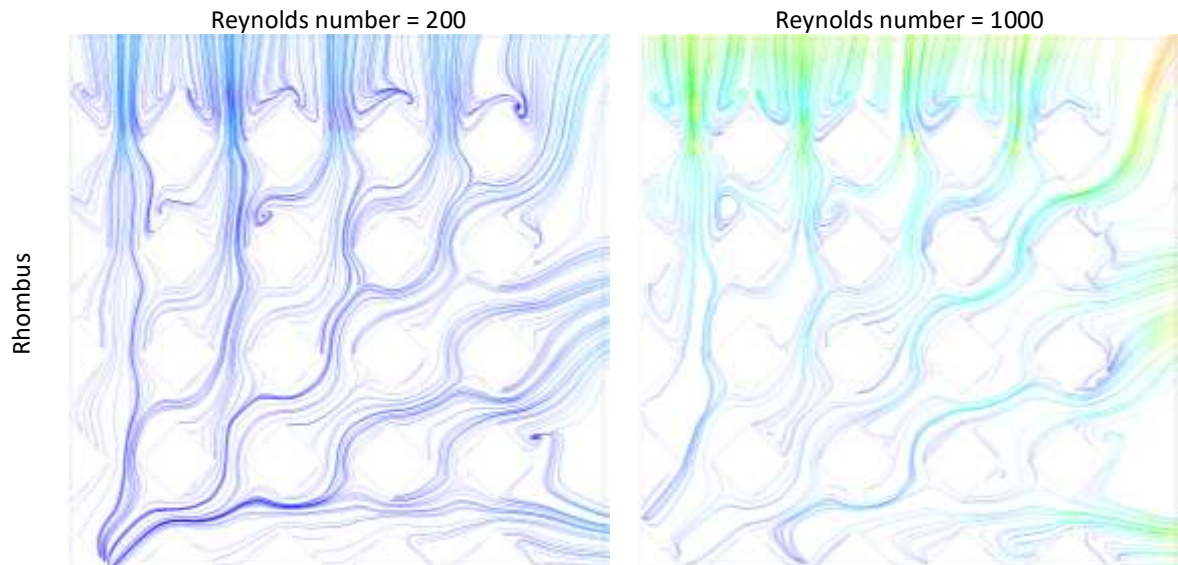


Fig. 12. Streamlines results gathered for rhombus shaped pin fin at Reynolds number 200 and 1000

3.3.4 Hexagon

In comparison with rhombus shaped pin fin, hexagon shaped pin also displays similar streamlines pattern that is turbulent. But it differs in terms of the formation of vortices and the uniformity of the streamlines as can be seen in Figure 13. Hexagon shaped pin fin shows less clustered streamlines which leads to more uniform flow. Despite that, the formation of vortices is still present although not as prominent as shown within rhombus shaped pin fin. The difference in both the streamline pattern and the vortices formation affects the overall performance of the heat sink as the hexagon shaped pin fin managed to yield the lowest maximum temperature despite having the second highest pressure drop amongst all the studied shape of pin fin. Similar results were also gathered by past studies [15, 20-22] where all of them found out that hexagonal pin fin, as compared to other shape of pin fin studied in each study, yield lowest thermal resistance through providing a significant advantage to enhance its heat transfer to achieve better cooling performance.

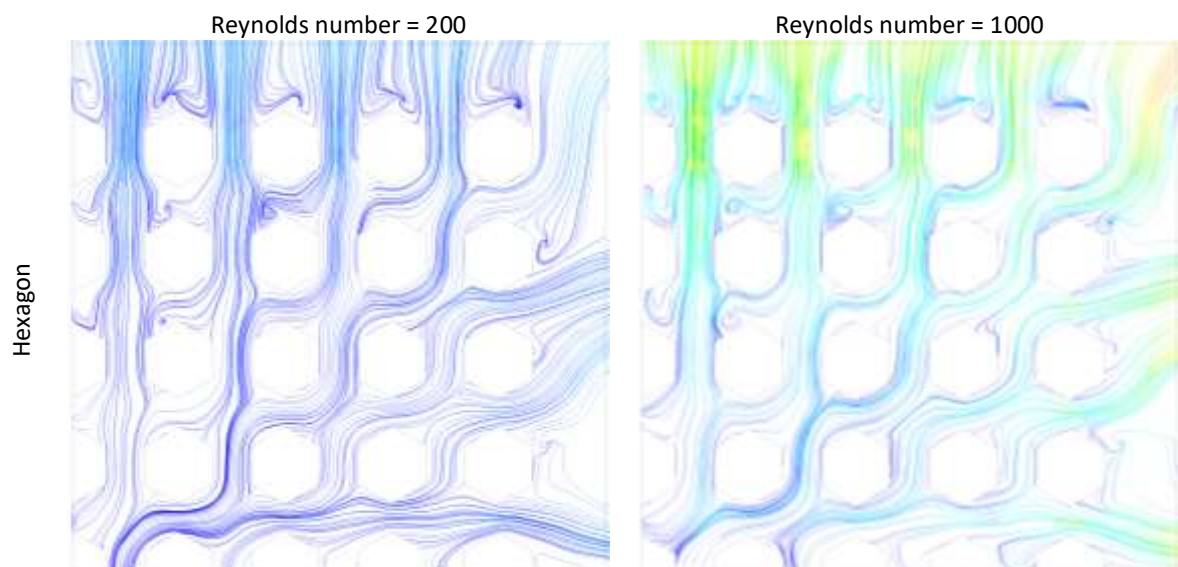


Fig. 13. Streamlines results gathered for hexagon shaped pin fin at Reynolds number 200 and 1000

4. Conclusions

Different geometry of pin fin within a microchannel heat sink under different Reynolds numbers were proposed in the study to observe the flow pattern within a crossflow condition of a heat sink. Based on the results gathered numerically, the conclusions of this study are.

- i) As the Reynolds number increases, the trend for the maximum temperature and the pressure drop are the same across the studied geometry which is decreasing and increasing respectively.
- ii) From the studied geometry, hexagon shaped pin fin yielded the lowest maximum temperature, whereas circular shaped pin fin yielded the lowest pressure drop.
- iii) From the flow pattern, it is observed that the balance between the formation of vortices and the turbulence of a flow within a heat sink is very important to achieve lower temperatures whilst still maintaining lower pressure drop.

Acknowledgement

Universiti Tun Hussein Onn Malaysia is providing financial assistance for this research under the UTHM GPPS Grant (Q221). The author expresses gratitude to the Faculty of Engineering Technology at Universiti Tun Hussein Onn Malaysia for facilitating the study with workable research facilities. Financial support from Universiti Tun Hussein Onn Malaysia and the UTHM Publisher's Office through Publication Fund E15216 enable the dissemination of the research.

References

- [1] Li, Zhaolong, Wangwang Li, Yingtao Liu, Meng Xun, and Mengchen Yuan. "Study of heat transfer performance of miniature heat sink for integrated circuit packaging field." *Case Studies in Thermal Engineering* 49 (2023): 103290. <https://doi.org/10.1016/j.csite.2023.103290>
- [2] Zubert, Mariusz, Tomasz Raszkowski, Agnieszka Samson, and Piotr Zając. "Methodology of determining the applicability range of the DPL model to heat transfer in modern integrated circuits comprised of FinFETs." *Microelectronics Reliability* 91 (2018): 139-153. <https://doi.org/10.1016/j.microrel.2018.07.141>
- [3] Jung, Daewoong, Haeun Lee, Daeyoung Kong, Eunho Cho, Ki Wook Jung, Chirag R. Kharangate, Madhusudan Iyengar et al. "Thermal design and management of micro-pin fin heat sinks for energy-efficient three-dimensional stacked integrated circuits." *International Journal of Heat and Mass Transfer* 175 (2021): 121192. <https://doi.org/10.1016/j.ijheatmasstransfer.2021.121192>
- [4] Abbas, T., K. M. Abd-Elsalam, and K. H. Khodairy. "CPU thermal management of Personal and notebook computer (Transient study)." In *2010 3rd international conference on thermal issues in emerging technologies theory and applications*, pp. 85-93. IEEE, 2010. <https://doi.org/10.1109/THETA.2010.5766383>
- [5] Japar, Wan Mohd Arif Aziz, Nor Azwadi Che Sidik, Rahman Saidur, Yutaka Asako, and Siti Nurul Akmal Yusof. "A review of passive methods in microchannel heat sink application through advanced geometric structure and nanofluids: Current advancements and challenges." *Nanotechnology Reviews* 9, no. 1 (2020): 1192-1216. <https://doi.org/10.1515/ntrev-2020-0094>
- [6] Ramesh, K. Naga, T. Karthikeya Sharma, and G. Amba Prasad Rao. "Latest advancements in heat transfer enhancement in the micro-channel heat sinks: a review." *Archives of Computational Methods in Engineering* 28 (2021): 3135-3165. <https://doi.org/10.1007/s11831-020-09495-1>
- [7] Du, Liang, and Wenbo Hu. "An overview of heat transfer enhancement methods in microchannel heat sinks." *Chemical Engineering Science* (2023): 119081. <https://doi.org/10.1016/j.ces.2023.119081>
- [8] Bhandari, Prabhakar, Kamal S. Rawat, Yogesh K. Prajapati, Diwakar Padalia, Lalit Ranakoti, and Tej Singh. "A review on design alteration in microchannel heat sink for augmented thermohydraulic performance." *Ain Shams Engineering Journal* 15, no. 2 (2024): 102417. <https://doi.org/10.1016/j.asej.2023.102417>
- [9] Zhang, Xuelai, Zhe Ji, Jifen Wang, and Xin Lv. "Research progress on structural optimization design of microchannel heat sinks applied to electronic devices." *Applied Thermal Engineering* (2023): 121294. <https://doi.org/10.1016/j.applthermaleng.2023.121294>

- [10] Loon, Yew Wai, and Yutaka Asako. "Numerical Analysis of Fluid Flow and Heat Transfer Characteristics of Novel Microchannel Heat Sink." *Journal of Advanced Research in Numerical Heat Transfer* 15, no. 1 (2023): 1-23. <https://doi.org/10.37934/arnht.15.1.123>
- [11] Dong, Wenlin, Xilong Zhang, Bilong Liu, Bin Wang, and Yubao Fang. "Research progress on passive enhanced heat transfer technology in microchannel heat sink." *International Journal of Heat and Mass Transfer* 220 (2024): 125001. <https://doi.org/10.1016/j.ijheatmasstransfer.2023.125001>
- [12] Ahmadian-Elmi, M., A. Mashayekhi, S. S. Nourazar, and K. Vafai. "A comprehensive study on parametric optimization of the pin-fin heat sink to improve its thermal and hydraulic characteristics." *International Journal of Heat and Mass Transfer* 180 (2021): 121797. <https://doi.org/10.1016/j.ijheatmasstransfer.2021.121797>
- [13] Ndao, Sidy, Yoav Peles, and Michael K. Jensen. "Effects of pin fin shape and configuration on the single-phase heat transfer characteristics of jet impingement on micro pin fins." *International Journal of Heat and Mass Transfer* 70 (2014): 856-863. <https://doi.org/10.1016/j.ijheatmasstransfer.2013.11.062>
- [14] Rao, Xixin, Cheng Jin, Haitao Zhang, Jianhao Song, and Chengdi Xiao. "A hybrid microchannel heat sink with ultra-low pressure drop for hotspot thermal management." *International Journal of Heat and Mass Transfer* 211 (2023): 124201. <https://doi.org/10.1016/j.ijheatmasstransfer.2023.124201>
- [15] Bhandari, Prabhakar, Diwakar Padalia, Lalit Ranakoti, Rohit Khargotra, Kovács András, and Tej Singh. "Thermo-hydraulic investigation of open micro prism pin fin heat sink having varying prism sides." *Alexandria Engineering Journal* 69 (2023): 457-468. <https://doi.org/10.1016/j.aej.2023.02.016>
- [16] Yang, Dawei, Yan Wang, Guifu Ding, Zhiyu Jin, Junhong Zhao, and Guilian Wang. "Numerical and experimental analysis of cooling performance of single-phase array microchannel heat sinks with different pin-fin configurations." *Applied Thermal Engineering* 112 (2017): 1547-1556. <https://doi.org/10.1016/j.applthermaleng.2016.08.211>
- [17] Lee, Minhyung, Gwanyong Park, Changyoung Park, and Changmin Kim. "Improvement of grid independence test for computational fluid dynamics model of building based on grid resolution." *Advances in Civil Engineering* 2020, no. 1 (2020): 8827936. <https://doi.org/10.1155/2020/8827936>
- [18] Qiu, Yunlong, Wenjie Hu, Changju Wu, and Weifang Chen. "An experimental study of microchannel and micro-pin-fin based on-chip cooling systems with silicon-to-silicon direct bonding." *Sensors* 20, no. 19 (2020): 5533. <https://doi.org/10.3390/s20195533>
- [19] Guan, Xiaonan, Zhihui Xie, Gang Nan, Kun Xi, Zhuoqun Lu, and Yanlin Ge. "Thermal–Hydrodynamic behavior and design of a microchannel pin-fin hybrid heat sink." *Micromachines* 13, no. 12 (2022): 2136. <https://doi.org/10.3390/mi13122136>
- [20] Roozbehi, Ahmad Reza, Mohammad Zabetian Targhi, Mohammad Mahdi Heyhat, and Ala Khatibi. "Modified hexagonal pin fins for enhanced thermal-hydraulic performance of micro-pin fin heat sinks." *International Journal of Numerical Methods for Heat & Fluid Flow* 33, no. 8 (2023): 2902-2926. <https://doi.org/10.1108/hff-02-2023-0053>
- [21] Kotcioglu, Isak, Gokhan Omeroglu, and Sinan Caliskan. "Thermal performance and pressure drop of different pin-fin geometries." *Hittite Journal of Science and Engineering* 1, no. 1 (2014): 13-20. <https://doi.org/10.17350/hjse19030000003>
- [22] Rezazad Bari, Amir, Mohammad Zabetian Targhi, and Mohammad Mahdi Heyhat. "A numerical study on thermo-hydraulic performance of micro pin-fin heat sink using hybrid pin-fins arrangement for electronic cooling devices." *International Journal of Numerical Methods for Heat & Fluid Flow* 33, no. 7 (2023): 2478-2508. <https://doi.org/10.1108/hff-10-2022-0608>